1973, *Astron. Astrophys. Suppl.* **12**, 331-350.

A SINGLE YOUNG OPEN CLUSTER COMPRISING Tr 14 AND Tr 16

A. FEINSTEIN*, H.G. MARRACO and J.C. MUZZIO
Observatorio Astronómico, Universidad Nacional de La Plata, Argentina

Received January 3, revised March 16, 1973

New photoelectric observations of the open cluster Tr 16, including faint members, and also many stars in and nearby the open cluster Tr 14 were obtained. Tr 16 surrounds the peculiar object η Car. Both clusters and Cr 232 seem to form a single group with very young characteristics. This agrees with the spectral type 03 of the brightest stars in the group as suggested by Walborn (1973).

The true distance modulus for the group of clusters, if it is assumed that $R=3.0$, is $12^m.65 \pm 0^m.20$, equivalent to a distance of $d=3390 \pm 300$ pc. But the $(V-I, B-V)$ array indicates that it is possible that $R=4.0$, in which case the corrected distance modulus is $12^m.12$, and the distance of the cluster group decrease to $d=2650$ pc. The age of the cluster group is about 3×10^6 years, which is slightly higher than that of the open cluster NGC 6611 used for the definition of the early part of the ZAMS.

An inspection of the plotted colour excess of each star in its own position in the emission nebula NGC 3372 shows that the clusters and η Car are associated with the dust. Finally it is suggested that there is a close spatial relationship between the emission nebula, the dust and the stars belonging to the cluster.

Key words: open cluster - *UBVRI* and Balmer line photometry - colour excess - dust - gas

1. INTRODUCTION

The open cluster Tr 16 which contains the very remarkable object η Car is located in one of the most prominent parts of the bright emission nebula NGC 3372. Two other open clusters Tr 14 and Cr 232 are located in the same region, about 12′ in diameter. Until now there is no agreement whether all of them are situated at different distances (Thé and Vleeming 1971; Walborn 1973), or whether they just form one physical group (Becker 1960).

The brightest stars located in this region are of very high luminosity. Thirteen of them were classified by Walborn (1971a, 1973) as of very early type; six are of spectral type O3V, and the remaining of slightly later types. This suggests the very young characteristics of this region.

Many stars around η Car were already observed photoelectrically and the results published in earlier papers (Feinstein 1963, 1969). Photographic measures were also published by Becker (1960), and lately more stars were included in the data listed by Thé and Vleeming (1971).

From these informations it is clear that the connection of the star η Car with the open cluster Tr 16 and the bright emission nebula NGC 3372 is not well established. But if we want to get some conclusions about this unique object, it must be very important to know with confidence the relation between all of them.

2. THE OBSERVATIONS

New photoelectric observations of 132 stars in the region of the open clusters Tr 14, Tr 16 and Cr 232 are reported in this paper. The *UBV* measures were carried out with the 36 and 60″ telescopes of the Cerro Tololo Inter-American Observatory, during April 1970 and February 1972; in the *RI* system 27 stars were observed in December 1968 with an RCA 7102 photomultiplier and *RI* filters (Feinstein 1966). The 80 cm telescope at La Plata Observatory was also employed during March, April and July 1972 for the *UBV* measures of the stars belonging to Tr 14.

*Visiting Astronomer, Cerro Tololo Inter-American Observatory, which is operated by the Association of Universities for Research in Astronomy, Inc., under contract with the National Science Foundation.

An identification chart of the Tr 16 region is given in figure 1, while in figure 2 the open cluster Tr 14 and Cr 232 are shown, separated by a line as suggested by Walborn (1973). Table 1 contains the *UBV* data for all the stars in this region. The root mean square error of one observation is for *V*, *B–V* and *U–B*, respectively, $\varepsilon_V = \pm 0^m.035$, $\varepsilon_{B-V} = \pm 0^m.025$ and $\varepsilon_{U-B} = \pm 0^m.030$. In the column giving the number of observations, headed by N, an asterisk means that the data for each particular star were already published (Feinstein 1969). A letter N indicates that a new observation was made, and that the mean of old and new values is given. If there is no indication at all the star was measured for the first time. The *RI* measurements are listed in Table 2. The root mean square error of one observation for *R* and *R–I* are $\varepsilon_R = \pm 0^m.04$ and $\varepsilon_{R-I} = \pm 0^m.03$ respectively.

3. COLOUR-MAGNITUDE AND COLOUR-COLOUR DIAGRAMS

All the data we have obtained for the 132 stars are plotted in the colour-magnitude diagrams: (*B–V, V*) and (*U–B, V*). (Figure 3 and 4), and in the colour-colour diagram (figure 5). The stars belonging to the clusters Tr 14 and Tr 16 are indicated by triangles and circles respectively in order that if they are situated at different distances it will become apparent. The small group known as Cr 232 consists of a few stars around HDE 303311 and HD 93250. Because some of them are nonmembers, it is not shown separately.

4. MEMBERSHIP

In order to decide upon membership in the clusters we divided the stars located in the colour-colour diagram (figure 5) in four groups:

a) The stars situated within the A–F–G dwarf intrinsic colour relation, the reddening line starting at G0 and to the right of the line parallel to the OB intrinsic colour relation drawn with $E(B-V) = 0^m.38$. (We shall call the second mentioned line the G0 reddening line). These stars are presumably OB members.

b) The stars lying above the A–F–G dwarf intrinsic colour relation and to the left of the line parallel to the intrinsic colour relation at $E(B-V) = 0^m.38$. These are presumably OB foreground stars.

c) The stars plotted within the region bounded by the dwarf A–F–G intrinsic colour relation, the G0 reddening line and A3 reddening line. Some OB members are expected to belong to this group and also some A–F–G foreground stars.

d) The two stars located far below the A3 reddening line and to the left of the G–K type intrinsic colour relation. The position of these stars (no. 79 of Tr 16 and no. 14 of Tr 14) marked with X in figure 9 can not be clearly explained; it is possible however that their observed colours are in error.

Using all the stars of group a) a preliminary corrected colour-magnitude diagram was drawn (see next section) assuming that all of them are OB dwarfs. Then a preliminary isocryptic chart was also drawn (see figure 9). Those stars which are located far above the main sequence and at the same time have smaller reddening than their neighbours in the sky are considered foreground nonmembers of OB type.

The stars of group b) were then checked and all of them turned out to be foreground stars.

If in group c) some contracting stars are present, they should have apparent magnitudes fainter than $V_0 = 9^m.7$. We shall now consider the OB stars in group c). If a star, supposed to be an OB dwarf, has a colour excess in accordance with their surrounding, and is at the same time close to the main sequence or fainter than $V_0 = 9^m.7$, then it is retained. A doubtful case is no. 49 in Tr 16 which has the lowest admitted excess for a member.

Star no. 29 in Tr 14 belonging to group a) has a colour excess that exceeds that of its neighbourhood. The corrected magnitude and colour of this star fit the main sequence well. It is thus not a background object, unless the absorption changes very suddenly behind this stellar aggregate. This conclusion can not be checked since we have detected no other background star except perhaps no. 22 in Tr 16. On the other hand, if we con-

sider the star to be a member, and no zonal absorption is apparent in long exposure pictures of the field, we may explain this fact by assuming that the star has a circumstellar shell. To this hypothesis we like to add the following remark: the star is not one of the brightest and cannot be among them, unless one admit $R=5.5$ for this region.

5. DISTANCE MODULUS AND AGE

In the preceding section we have applied a preliminary corrected colour-magnitude diagram, which is obtained using the following data and assumptions.

The observed UBV data indicate that all the member stars are very probably OB dwarfs or giants. This agrees with Walborn's (1972) spectra of the brightest members showing very early characteristics. The intrinsic colour-colour relation of the OB dwarfs and giants is given by the linear equation

$$(U-B)_0=3.69\,(B-V)_0+0^m.03,$$

and the ratio of colour excesses by

$$E(U-B)/E(B-V)\rightarrow=0.69+0.05\,E(B-V).$$

Using these formulas the intrinsic colours $(B-V)_0$, $(U-B)_0$ and the colour excesses E_{B-V}, E_{U-B} were computed in a way explained by Feinstein and Marraco (1971). The employed zero age main sequence (ZAMS) is that of Blaauw (1963), and the adopted ratio of total to selective absorption is

$$R=A_V/E(B-V)=3.0.$$

With the last assumption the magnitude of the members and the foreground OB stars were individually corrected for absorption.

The corrected modulus for each star, if it is unevolved or has already finished its contracting phase, was computed by taking into account the absolute magnitude read from the ZAMS (that is the M_V° value) at the corresponding intrinsic colours. This data, which include that of some foreground stars, are listed in Table 3. A final corrected colour-magnitude diagram is then presented in figure 6.

Using these data and the standard mean evolutionary deviation curve taken from figure 4 of Lindoff (1968), we have made a simultaneous horizontal and vertical adjustment.

From the vertical fit a corrected modulus of

$$V_0-M_V=12^m.65\pm0^m.20$$

was obtained, corresponding to a distance of 3.39 ± 0.30 kpc. In this vertical fit allowance was made for duplicity, since this very frequent phenomenon among OB stars can brighten the star up to $0^m.75$, reducing the distance modulus in the corresponding amount.

It was assumed a 55% of double stars distributed uniformly in magnitude between $\Delta m=0^m.0$ and $0^m.75$ ($\Delta m=$ true less observed modulus). When this was combined with the usually adopted $0^m.5$ dispersion in the absolute magnitudes due to uncertainties in the determination of the intrinsic colours, we found that the resulting distribution would have only 35% of the stars with distance moduli greater than the true modulus. On the other hand the range $-0^m.8<\Delta m<1^m.3$ contains 95% of the members while the mode of the distribution is about $\Delta m=0^m.25$.

Then we have adjusted the mean evolutionary deviation curve to meet all the above mentioned requirements and explained at the same time that outside the already mentioned range of about $2^m.1$ for the distance moduli we have admitted only 5 non-contracting members stars, that is less than 5%.

From the horizontal fit and using the upper margin of figure 8 it is possible to compare the characteristics of our cluster with the isochrones given in Lindoff (figure 3, Lindoff 1968). It is clear that Tr 14-16 is definitely younger than 5×10^6 years. For comparison purposes we have reduced Walker's (1961) data

of NGC 6611 in exactly the same procedure as Tr 14-16 and plotted the results in figure 7 as a corrected colour-magnitude diagram. A comparison of figure 6 and 7 shows that NGC 6611 is somewhat younger than Tr 14-16; a conclusion drawn from the fact that the former has no evolved stars from the ZAMS, which is actually partly defined by itself. Walker gives 2×10^6 years for the age of NGC 6611, but the scale of his age is not in the same system as that of Lindoff.

In figures 8 and 9 of Lindoff's paper it is shown that his scale gives up to 10 times larger ages for clusters to which other authors assign an age of 10^6 years. This makes the problem worse and indicates that Walker's data of NGC 6611 may be at least 4×10^6 years in Lindoff's scale. We prefered therefore to assign more weight to the comparison with Lindoff's isochrones than to the age of NGC 6611, and thus adopted 3×10^6 years in Lindoff's scale for the age of Tr 14-16.

At the other end of the main sequence we can see that some stars appear as stars which are still in the process of contracting to the main sequence, but again a comparison with NGC 6611 shows that Tr 14-16 is somewhat older. The contracting stars in NGC 6611 reach the main sequence at $(U-B)_0=-0^m.80$, while in Tr 14-16 we find stars arriving already at the ZAMS at $(U-B)_0=-0^m.55$. Considering the closeness of this point to the observational limit, it is possible that this point is actually lying at redder colours.

6. THE DISTRIBUTION OF THE COLOUR EXCESS E_{B-V} IN THE η CAR REGION

As was explained before, from the observed $B-V$ and $U-B$, individual colour excesses are obtained for each star. It is interesting to investigate whether the distribution of the colour excesses of the 112 stars, which are very probably members of the cluster, have some relation to the location of the star.

In figure 9 a reproduction of a short exposure plate of the η Car region taken with the Curtis Schmidt telescope at Cerro Tololo, the values of the colour excesses $E(B-V)$ are given at the position of each star. Lines joining equal values of $E(B-V)$ are also drawn. For comparison purposes a yellow plate of the same region which shows the bright nebula NGC 3372 is depicted in figure 10.

In figure 11 the colour excesses are plotted against the corrected distance moduli. Assuming that the foreground stars are main sequence objects, from the diagram it is clear that at least $0^m.40$ of the colour excess is caused by the interstellar matter between the stellar aggregate and the sun. The spread in distance modulus shown by the cluster members is primarily due to uncertainties in the determination of intrinsic colours and also to duplicity, because we have already eliminated from the diagram all the evolving and contracting stars.

Looking again at figure 9 several interesting results can be derived:

a) The object η Car is at the place of the lowest excess colour ($E(B-V)=0^m.40$), surrounded by nearly circular lines of increasing absorption going further away. The diameter of this structure is about 2′, which at a distance of 3.39 kpc means of the order of 2 pc.

b) Another minimum of colour excess surrounds the stars HD 93204/5. Both of them are of very early spectral type O5V and O3V according to Walborn (1973).

c) To the north west of η Car, in a circular optical ring of low nebulosity, about 3′ in diameter, and known as the "key hole", the 4 stars inside it have very large colour excesses ($E(B-V)=0^m.72$).

d) A small dark patch, to the north west of the ring structure is correlated to large $E(B-V)$ values. The two stars nos. 10 and 12 inside it have colour excesses of $0^m.59$ and $0^m.62$ respectively.

The small value of the colour excess ($E(B-V)=0^m.40$) at the position of η Car indicates that this particular object is active in the sense that it is blowing away all the dust by radiation pressure.

The place of the region mentioned in c) agrees quite well with the centre of a strong radio continuum, measured at 6 cm by Gardner *et al.* (1970), and known as Car II. Star no. 30 located south west of the nucleus of Tr 14, and nearly at the centre of the other strong radio emission, Car I, shows also a large value of the interstellar absorption, as it has $E(B-V)=0^m.81$.

7. THE BRIGHTEST STARS

In figure 12 a reproduction of the brightest part of the intrinsic colour versus the corrected magnitude diagram of figure 3 is given. The known spectral type of each star, with the letter O omitted, is given at its position in the diagram.

The brightest stars are of very early spectral type (O3 and O5). The two very bright stars of spectral type O6 are slightly more evolved than the others. One of them is a binary (HD 93161). All this suggests a good correlation between the spectral types and the magnitudes for the most luminous stars of Tr 14-16.

It is apparent from the colour excess map (figure 9) that the brightest stars are always situated in zones of low reddening. This is the case for η Car, already mentioned, HD 93250, 93129, 93204, 93205 and HDE 303308 which all have colour excesses smaller that $0^m.51$. An exception is the Wolf-Rayet star HD 93162 with a colour excess of $0^m.75$. The intrinsic colours of this star are unknown but they must not be very far from those assigned by our reduction method. We obtained $E(B-V)=0^m.75$ and this value is used in the figures, but the true excess is surely about $0^m.6$ (Smith 1968, Walborn 1972). All this indicates that the bulk of the dust is associated with Tr 14 and Tr 16. In figure 13 the excess for each star is plotted against corrected visual magnitude. The brightest stars, with the exception of the WR star, have all small reddening. This cluster does not show the effect found by Reddish (1967) in other aggregates of ages 5×10^6 years or younger, namely the correlation between colour excess and luminosity. It is interesting to note that the only bright star which was not able to blow away the dust shows the WR phenomenon.

Photoelectric measures with interference filters of the Balmer lines: Hα, Hβ, and Hγ were obtained after a long investigation of the emission of the hydrogen lines in early-type stars. In table 4 these measures of 12 stars of Tr 16 are listed. The Hβ values are in the Crawford and Mander system (1966). On the other hand the Hα and Hγ observations are given in a new defined system (Feinstein 1973). We find that only the stars HD 93250 and 93205 have faint Hα emission, the others have no measurable emission at all. We therefore conclude that with these two exceptions all the other stars have normal characteristics, at least with respect to the hydrogen lines.

8. THE η CAR OBJECT

The amount of interstellar reddening for the stars around η Car shows that in its surrounding region there is a lack of dust, with a minimum just in the direction of this peculiar object. The external colour excess of η Car is about $E(B-V)=0^m.40$ (figure 9), which is due mostly to the dust distributed regularly between it and the sun. No influence of the dust just in front of the cluster members is apparent.

From the work of Pagel (1969) and Ade and Pagel (1970), it was deduced that the colour excess obtained from the relative intensities of the FeII and [FeII] lines of its spectrum is $E(B-V)=1^m.2$. This value refers to the total absorption of the dust between the star and the Earth.

The difference of colour excess between these two values ($0^m.40$ and $1^m.2$) is related to the dust just around the star, which has a shape resembling a homunculus (Gaviola 1946, 1950; Thackeray 1949; Gehrz and Ney 1972). A similar assumption is used in the work of Schmidt (1971).

Assuming the following characteristics for the physical data of the object η Car:

Data		*Explanation*
$E(B-V)=0^m.8$		Colour excess caused by the dust in the homunculus.
d	$=3.39$ kpc	Adopted distance of η Car.
R	$=3.0$	Adopted ratio of total to selective absorption for the dust in the homunculus.
a	$=6''.5$	Major axis of the homunculus.
b	$4''.0$	Minor axis of the homunculus.
κ_V	$=2.45\times10^4$ cm^2 gr^{-1}	Adopted mass absorption coefficient (Spitzer 1968).

Then one obtains the following results:

Results	*Explanation*
$a' = 0.11$ pc	Major axis of the homunculus.
$b' = 0.07$ pc	Minor axis of the homunculus.
$\frac{m}{m_\odot} = 4.74 \times 10^3 \frac{u\pi}{3} \frac{a'b'R\,E(B-V)}{1.086\,\kappa_V} = 0.014$	Total mass of the dust in the homunculus in the direction to the Sun.

As it is normally accepted that the ratio of the gas to the dust is around 100, we can conclude that the total mass of the circumstellar gas around η Car is approximately 1 solar mass. This suggests that the central star is very massive, which confirms early assumptions about the structure of this particular star (Burbidge 1962).

9. THE LAW OF INTERSTELLAR REDDENING

In the $(V-I, B-V)$ array (figure 14) the 24 member stars of early types observed in the RI system are plotted. In this diagram the solid line is the main sequence according to Johnson (1966), and the dashed lines are the paths of interstellar reddening for

$$E(V-I)/E(B-V) = 1.62 \text{ and } E(V-I)/E(B-V) = 2.50$$

respectively. The first line is the normal extinction curve which corresponds to $R=3$; the second one to $R=5$, similar to the region of the Orion Sword. Both values were taken from Johnson (1968).

The cluster stars plotted in figure 14 are the brightest ones. The intrinsic colours $(B-V)_0$ are about the same for all of them (see table 3), with a mean value of $(B-V)_0 = -0^m.32$ and a range of $-0^m.33 < (B-V)_0 < -0^m.25$.

The distribution of the points in figure 14 suggests that the correct R value for this region is between 3 and 5. Thus the η Car region has a slightly larger ratio of total to selective absorption than normal. Consequently the distance of the cluster should be decreased.

Assuming a value of $R=4.0$ we obtain a corrected distance modulus of $V_0 - M_V = 12^m.12$, which corresponds to a distance of $d=2650$ pc.

10. RELATION AMONG STARS, DUST AND GAS

There is a good agreement between the optical absorption and the large amount of dust derived from the excess $E(B-V)$ of the stars in the remarkable ringshaped region and in a few other areas. This confirms the fact that some large irregular concentration of interstellar dust should be located in front of the stars, which we can see as dark patches against the bright nebula NGC 3372. On the other hand an expanding ring of gas surrounding η Car is apparent from the hydrogen H 109α recombination line (Gardner, Milne, Mezger and Wilson 1970), which may be due to the nova like phenomenon that took place slightly more than a century ago. This suggests that the gas is associated to η Car. All these correlations and the lack of dust around η Car and the brightest stars, give a good evidence of the interconnection between stars, gas and dust in this particular region.

ACKNOWLEDGEMENT

One of us (A.F.) wishes to express his special acknowledgement to the Cerro Tololo Inter-American Observatory for the use of its facilities. This work was done by H.G. Marraco while having fellowship from the Consejo National de Investigaciones Cientificas y Técnicas, Argentina. A large part of the observations were obtained by A. Feinstein during a tenure of a John Simon Guggenheim Memorial Fellowship, and was also partially supported by a contract with the Consejo Nacional de Investigaciones.

REFERENCES

Ade, P. Pagel, B.E.J.: 1970, *Observatory* **90**, 6.
Becker, W.: 1960, *Z. Astrophys.* **51**, 49.
Blaauw, A.: 1963, in K. Aa. Strand (ed.), *Basic Astronomical Data,* University of Chicago Press, p. 383.
Burbidge, G. R.: 1962, *Astrophys. J.* **136**, 304.
Crawford, D.L. and Mander, J.: 1966, *Astron. J.* **71**, 114.
Feinstein, A.: 1963, *Publ. Astron. Soc. Pacific* **75**, 492.
Feinstein, A.: 1966, *Inf. Bull. of the Southern Hemisphere* no. 8, 30.
Feinstein, A.: 1969, *Monthly Notices Roy. Astron. Soc.* **143**, 273.
Feinstein, A.: 1973, *IAU Symp.* no. 50, (in press).
Feinstein, A. and Marraco, H.G.: 1971, *Publ. Astron. Soc. Pacific* **83**, 218.
Gardner, F.F. Milne, D.K., Mezger, P.G., and Wilson, T.L.: 1970, *Astron. Astrophys.* **7**, 349.
Gaviola, E.: 1946, *Nature* **158**, 403.
Gaviola, E.: 1950, *Astrophys. J.* **111**, 408.
Gehrz, R.D. and Ney, E.P.: 1972, *Sky Telesc.* **41**, 4.
Johnson, H.L.: 1966, *Ann, Rev. Astron. Astrophys.* **4**, 193.
Johnson, H.L.: 1968, in B.M. Middlehurst and L.H. Aller (eds.), *Nebulae and Interstellar Matter*, University of Chicago Press, p. 167.
Lindoff, U.: 1968, *Arkiv Astron.* **5**, 1.
Pagel, B.E.J.: 1969, *Nature* **221**, 325.
Reddish, V.C.: 1967, *Monthly Notices Roy. Astron. Soc.* **135**, 251.
Schmidt, Th.: 1971, *Astron. Astrophys.* **12**, 456.
Smith, L.: 1968, *Monthly Notices Roy Astron. Soc.* **140**, 417.
Spitzer, L.: 1968, *Diffuse Matter in Space,* Interscience Publishers, p. 69.
Thé, P.S. and Vleeming, G.: 1971, *Astron. Astrophys.* **14**, 220.
Thackeray, A.D.: 1949, *Observatory* **69**, 31.
Walborn, N.R.: 1971a, *Astrophys. J.* **167**, L31.
Walborn, N.R.: 1971b, *Publ. Astron. Soc. Pacific* **83**, 811.
Walborn, N.R.: 1973, *Astrophys. J.* **179**, 517.
Walker, M.F.: 1961, *Astrophys. J.* **133**, 438.

A. Feinstein
H.G. Marraco
J.C. Muzzio

Observatorio Astronómico
Universidad Nacional de La Plata
Paseo del Bosque
La Plata, Argentina

Table 1 *UBV* observations in the η Car region

TRUMPLER 16

HD/NO.	V	B-V	U-B	N	SP. T./REMARKS
93250	7.37	0.16	-0.85	8N	O3V((F))
93205	7.75	0.05	-0.91	3*	O3V
93160	7.82	0.17	-0.77	2	O6III(F)
93161AB	7.82	0.21	-0.70	2	O6.5V((F))
93162	8.10	0.41	-0.65	6*	WN6-A
303308	8.17	0.12	-0.84	8N	O3V
93204	8.42	0.10	-0.89	4*	O5V
100	8.61	0.21	-0.78	7*	O6V((F))
104	8.77	0.14	-0.79	3*	O7V((F))
303311	9.05	0.13	-0.86	4*	
112	9.29	0.32	-0.72	5*	
34	9.31	0.23	-0.77	2*	
110	9.31	0.31	-0.69	3*	
93268	9.32	0.10	0.05	2*	FOREGROUND
36	9.44	1.64	2.05	4N	
93343	9.47	0.29	-0.75	3*	
1	9.53	0.10	-0.80	5N	
19	9.78	0.33	-0.65	2*	
9	9.79	0.23	-0.71	6N	
10	9.83	0.30	-0.69	2*	
35	9.85	1.14	1.02	1*	
94	9.86	0.14	-0.62	4*	FOREGROUND
23	9.97	0.38	-0.64	3*	
115	10.15	0.16	-0.82	4*	
3	10.17	0.21	-0.75	5N	
20	10.20	0.08	-0.59	3*	FOREGROUND
31	10.44	0.27	-0.67	3*	
127	10.70	0.35	-0.55	2	
64	10.72	0.10	-0.74	2	
13	10.76	0.22	-0.61	3N	
2	10.80	0.14	-0.73	4N	
5	10.83	0.24	-0.67	2*	
16	10.87	0.24	-0.58	2*	VAR 10.75-11.00
8	10.90	0.14	-0.78	5*	
21	10.93	0.47	-0.54	3*	

TRUMPLER 16

HD/NO.	V	B-V	U-B	N	SP. T./REMARKS
126	10.97	0.41	-0.47	3	
4	11.00	0.25	-0.62	5N	DOUBLE
17	11.01	0.24	-0.74	2*	
22	11.01	0.49	-0.60	3*	
32	11.05	0.23	0.14	3*	FOREGROUND
27	11.06	0.14	-0.68	3N	
65	11.09	0.14	-0.65	2	
124	11.13	0.24	-0.65	2	
30	11.17	1.06	1.20	2*	
76	11.19	0.42	-0.57	2	
11	11.25	0.16	-0.66	2*	
15	11.28	0.41	-0.54	3N	
122	11.32	0.20	-0.57	2	
29	11.36	0.42	-0.47	3N	
12	11.44	0.30	-0.62	3N	
14	11.50	0.42	-0.56	3N	
129	11.57	0.38	-0.28	2	
24	11.58	0.16	-0.63	3*	
6	11.65	0.18	-0.49	3*	
25	11.66	0.24	-0.40	4N	
74	11.70	0.27	-0.60	2	
28	11.70	0.27	-0.58	3N	VAR 11.60-11.98
46	11.71	0.34	-0.37	2	
33	11.83	0.27	-0.51	2*	
26	11.89	0.26	-0.63	4N	
73	11.90	0.42	-0.46	2	
48	11.94	0.19	0.07	2	FOREGROUND
66	11.98	0.16	-0.57	2	
18	12.04	0.23	-0.60	4N	
77	12.08	0.27	-0.41	3	
72	12.10	0.24	-0.53	1	
80	12.14	0.40	-0.31	2	
125	12.15	0.65	-0.04.	3	FOREGROUND
78	12.19	1.09	1.31	1	
55	12.22	0.23	-0.53	1	
43	12.23	0.54	0.08	1	

Table 1 *(continued)*

TRUMPLER 16

HD/NO.	V	B-V	U-B	N	SP. T./REMARKS
41	12.30	0.26	-0.40	1	
59	12.36	0.20	-0.54	1	
61	12.40	0.21	-0.41	1	
58	12.42	0.23	0.21	1	FOREGROUND
60	12.47	0.19	-0.40	1	
68	12.48	0.21	-0.41	2	
52	12.58	0.37	-0.31	1	
123	12.59	0.22	-0.41	3	
130	12.72	0.30	-0.34	4	
42	12.74	0.34	-0.33	1	
40	12.79	0.40	-0.29	1	
63	12.82	0.27	-0.32	1	
39	12.82	0.45	-0.21	1	
54	12.85	0.38	-0.33	1	
51	12.89	0.33	-0.42	1	
57	12.90	0.37	-0.08	1	
47	12.91	0.34	-0.31	1	
50	12.92	0.30	-0.27	1	
37	12.95	0.24	-0.30	2	
69	13.03	0.36	0.28	2	FOREGROUND
45	13.03	0.70	0.18	1	
53	13.26	1.33	2.14.	1	
38	13.37	0.24	-0.26	1	
70	13.41	0.31	-0.31	2	
56	13.43	0.33	0.03	1	FOREGROUND
131	13.48	0.32	-0.30	3	
49	13.48	0.32	0.18	2	
71	13.65	0.38	-0.21	1	
44	13.67	0.53	-0.14	1	
79	13.68	0.45	0.60	1	
67	13.70	0.81	0.31	1	FOREGROUND
62	13.90	0.27	-0.10	1	
75	14.26	0.64	0.41	1	

TRUMPLER 14

HD/NO.	V	B-V	U-B	N	SP. T./REMARKS
93129AB	6.97	0.16	-0.78	1	O3IF*+O3V((F))
93128	8.84	0.25	-0.74	3	O3V((F))
8	9.40	0.17	-0.75	2	O6.5V((F))
20	9.61	0.28	-0.73	7	
9	9.92	0.21	-0.72	2	
30	10.08	0.50	-0.53	1	
3	10.80	0.26	-0.65	1	
21	10.88	0.34	-0.63	3	
4	11.08	0.24	-0.68	4	
6	11.23	0.19	-0.68	4	
27	11.32	0.30	-0.56	2	
5	11.41	0.33	-0.59	4	
19	11.58	0.34	-0.42	2	VAR 11.48-11.69
26	11.93	0.37	-0.57	7	VAR 11.80-12.11
29	11.97	0.50	-0.33.	3	VAR 11.89-12.03
15	12.01	0.30	-0.15	2	
24	12.12	0.37	-0.49	3	
7	12.12	0.32	-0.45	2	VAR 11.45-12.79
18	12.15	0.27	-0.59	4	
22	12.34	0.32	-0.48	2	
10	12.48	0.27	-0.50	1	
28	12.50	0.39	-0.53	2	
14	12.62	0.23	0.37	2	
13	12.63	0.24	-0.40	2	
12	12.64	0.24	-0.48	1	
17	12.65	0.29	-0.32	2	
11	12.78	0.39	0.05	6	VAR 12.58-13.01
25	12.88	0.32	-0.20	5	VAR 12.64-13.08
16	13.60	0.27	-0.27	1	

Table 2 RI measures of Tr 16

HD/NO.	R	R-I	N
93205	7.56	0.10	1
93162	7.41	0.68	2
303308	7.92	0.17	3
93204	8.20	0.28	1
100	8.28	0.32	3
104	8.62	0.17	1
303311	8.92	0.32	1
112	8.80	0.43	1
34	8.93	0.35	1
110	8.75	0.54	1
93268	9.19	0.07	1
36	8.23	1.01	2
93343	9.17	0.41	1
1	9.25	0.20	2
19	9.36	0.38	1
9	9.47	0.48	1
10	9.48	0.45	3
35	9.11	0.59	1
94	9.67	0.28	2
23	9.39	0.53	2
115	9.79	0.20	1
20	10.00	0.16	2
31	10.15	0.34	1
13	10.43	0.53	1
2	10.70	0.27	1
8	10.57	0.00	1
17	10.39	0.46	1

Table 3 Colour excesses, corrected visual magnitudes and distance modulus of member stars and OB non-member stars

Star		E_{B-V}	V_o	$V_o-M_V^o$	
Tr 16	93250	0.49	5.89	10.88	
	93205	0.38	6.62	11.06	
	93160	0.48	6.38	9.97	
	93161	0.51	6.30	9.59	
	303308	0.44	6.85	10.83	
	93204	0.43	7.12	11.56	
	100	0.53	7.01	11.00	
	104	0.45	7.42	11.01	
	303311	0.46	7.67	12.11	
	112	0.65	7.34	11.78	
	34	0.56	7.65	12.08	
	110	0.63	7.43	11.41	
	93268	0.10	9.00	7.50	Foregr.
	93343	0.62	7.60	12.04	
	1	0.40	8.33	11.62	
	19	0.64	7.86	11.45	
	9	0.53	8.19	11.78	
	10	0.62	7.98	11.97	
	94	0.40	8.69	10.77	Foregr.
	23	0.70	7.87	11.86	
	115	0.48	8.70	12.80	
	3	0.52	8.60	12.19	
	20	0.31	9.28	10.97	Foregr.
	31	0.57	8.73	12.02	
	127	0.63	8.81	11.65	
	64	0.38	9.57	12.41	
	13	0.49	9.30	11.88	
	2	0.43	9.51	12.60	
	5	0.53	9.23	12.32	
	16	0.50	9.36	11.70	Variable
	8	0.45	9.56	13.15	
	21	0.78	8.60	12.18	

Table 3 *(continued)*

Star	E_{B-V}	V_o	$V_o-M_V^o$	
126	0.68	8.93	11.52	
4	0.53	9.41	12.25	
17	0.56	9.34	13.33	
22	0.82	8.54	13.06	
32	0.25	10.30	8.90	Foregr.
27	0.41	9.82	12.41	
65	0.40	9.88	12.22	
124	0.53	9.55	12.64	
76	0.72	9.01	12.60	
11	0.43	9.96	12.55	
15	0.70	9.17	12.26	
122	0.45	9.97	12.06	
29	0.69	9.29	11.87	
12	0.59	9.66	12.75	
14	0.72	9.33	12.62	
129	0.58	9.84	10.93	
24	0.42	10.32	12.66	
6	0.40	10.46	11.95	
25	0.44	10.34	11.42	
74	0.55	10.06	12.90	
28	0.54	10.08	12.67	Variable
46	0.56	10.04	11.53	
33	0.52	10.28	12.37	
26	0.54	10.26	13.34	
73	0.69	9.84	12.42	
48	0.22	11.28	9.93	Foregr.
66	0.40	10.78	12.67	
18	0.50	10.55	13.14	
77	0.48	10.63	11.92	
72	0.49	10.64	12.73	
80	0.61	10.30	11.59	
55	0.47	10.80	12.69	
43	0.66	10.25	9.85	
41	0.47	10.90	12.19	
59	0.44	11.04	12.93	
61	0.41	11.18	12.27	
60	0.38	11.33	12.27	
68	0.41	11.26	12.35	
52	0.57	10.86	11.95	
123	0.42	11.33	12.42	
130	0.50	11.23	12.32	
42	0.54	11.11	12.20	
40	0.60	10.98	12.26	
63	0.45	11.46	12.20	
39	0.64	10.90	11.84	
54	0.59	11.07	12.36	
51	0.56	11.21	12.89	
57	0.50	11.41	11.25	
47	0.54	11.30	12.39	
50	0.47	11.50	12.04	
37	0.41	11.73	12.27	
69	0.36	11.95	10.40	Foregr.
45	0.83	10.56	10.25	
38	0.39	12.19	12.38	
70	0.50	11.91	12.85	
56	0.41	12.20	11.40	Foregr.
131	0.51	11.96	12.89	
49	0.35	12.43	11.08	
71	0.55	11.99	12.53	
44	0.72	11.52	12.46	
62	0.38	12.77	12.31	
75	0.67	12.25	10.90	

Table 3 *(continued)*

	Star	E_{B-V}	V_o	$V_o-M_V^o$	
Tr 14	93129	0.47	5.54	9.13	
	93128	0.57	7.13	11.12	
	8	0.47	7.98	11.27	
	20	0.60	7.80	11.69	
	9	0.51	8.38	11.67	
	30	0.81	7.63	11.22	
	3	0.55	9.14	12.23	
	21	0.64	8.94	12.53	
	4	0.54	9.47	12.76	
	6	0.47	9.81	12.90	
	27	0.57	9.61	12.19	
	5	0.62	9.55	12.64	
	19	0.57	9.88	11.57	Variable
	26	0.64	9.96	12.80	Variable
	29	0.74:	9.74	11.82	Variable
	15	0.43	10.71	10.55	
	24	0.64	10.22	12.80	
	7	0.56	10.44	12.33	Variable
	18	0.54	10.52	13.11	
	22	0.57	10.63	12.72	
	10	0.51	10.94	12.83	
	28	0.67	10.48	13.32	
	13	0.44	11.30	12.39	
	12	0.47	11.23	12.92	
	17	0.48	11.22	12.16	
	11.	0.48	11.35	10.64	Variable
	25	0.47	11.46	11.65	Variable
	16	0.43	12.30	12.70	

Table 4 Photoelectric H_α, H_β, and H_γ measures in Tr 16

HD	H_α	H_β	H_γ	n
93250	1.401	2.553	2.039	1
93205	1.423	2.568	2.049	1
303308	1.441	2.539	2.052	1
93204	1.487	2.504	2.033	1
100	1.527	2.549	2.053	1
104	1.469	2.528	2.078	1
112	1.509	2.637	2.116	1
34	1.438	2.566	2.065	1
110	1.448	2.544	2.066	2
93268	1.475	2.713	2.297	1

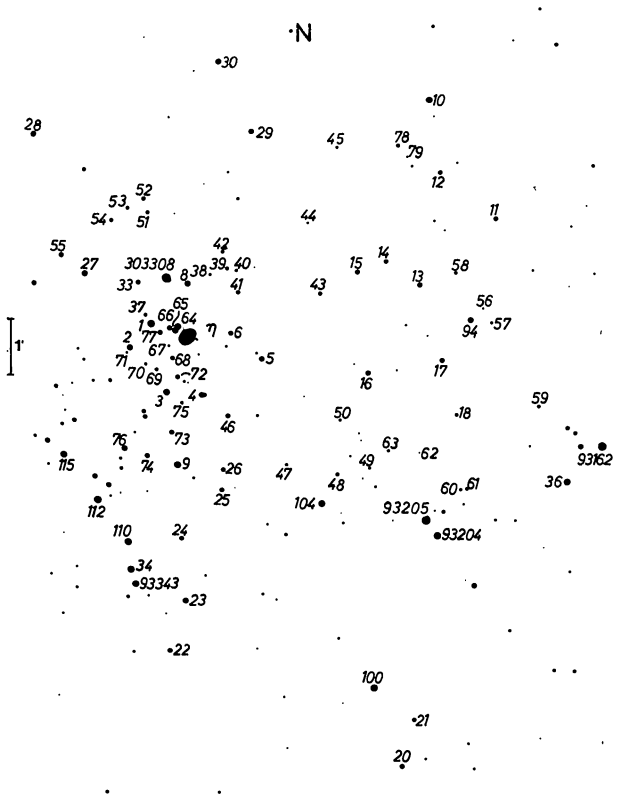

Figure 1 Identification chart for the region of Tr 16. The star η Car is somewhat to the left of the centre.

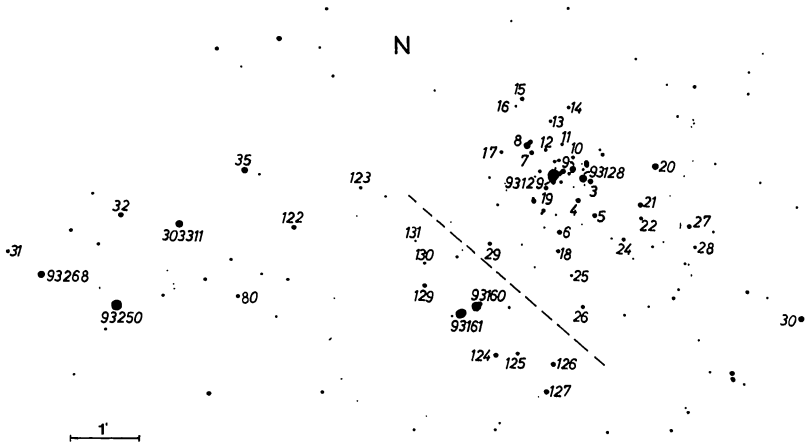

Figure 2 Identification chart for the region of Tr 14 and Cr 232. The stars to the right and above the dashed line are assumed here to form the Tr 14 group, and that those to the left and below this line belong to the Tr 16 aggregate. The sparse group of stars near HD 93250 is known as Cr 232 and is not considered as a separate system.

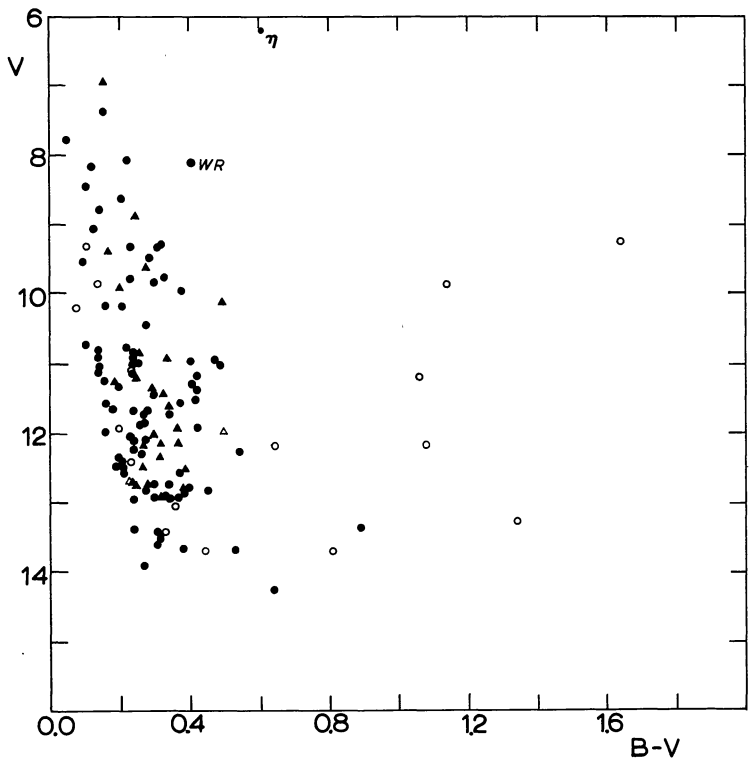

Figure 3 The observed *B–V* colour-magnitude diagram. Triangles and circles indicate stars in the zones of Tr 14 and Tr 16 respectively. Filled symbols stand for those stars considered to be members.

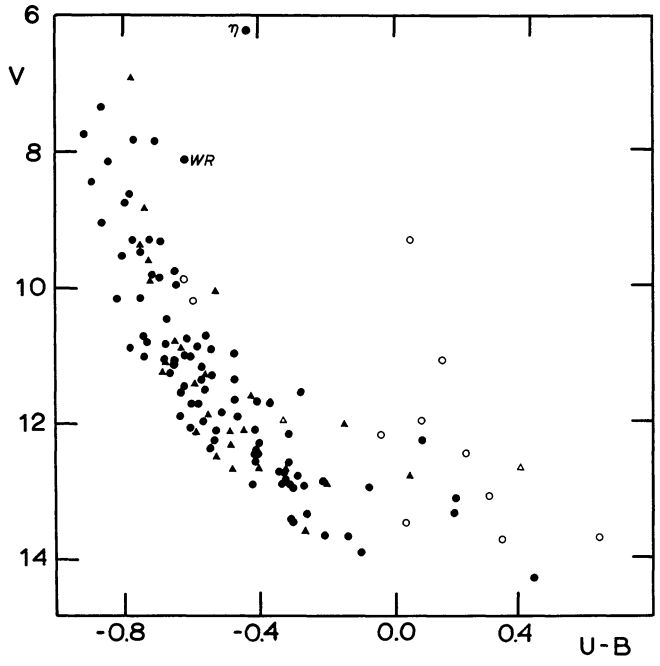

Figure 4 The observed *U–B* colour-magnitude diagram. The symbols have the same meaning as in figure 3. Only the blue part of the diagram is shown. Note that non-member stars are here more easily separeted than in figure 3.

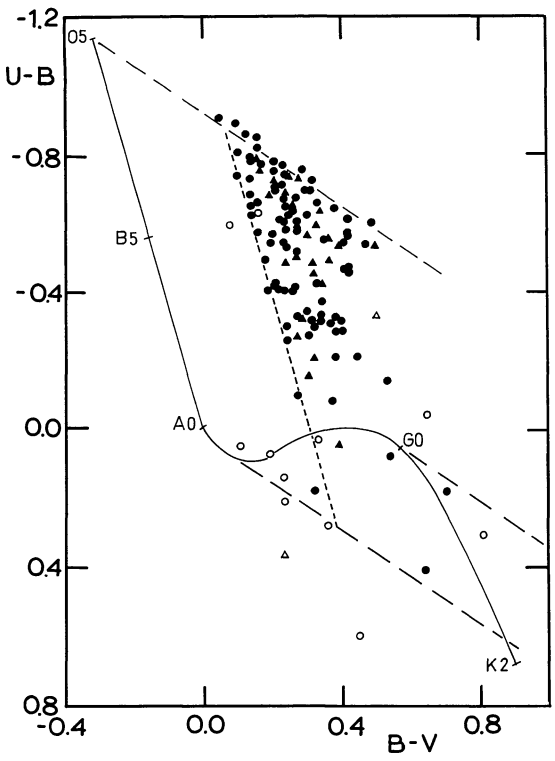

Figure 5 The colour-colour diagram. The symbols have here also the same meaning as in figure 3. Only the blue part of the diagram is shown. The intrinsic colour-colour relation for dwarfs is drawn as a full line and labeled with spectral types. Reddening lines with a slope of $E_{U-B}/E_{B-V}=0.69$ are drawn as dashed lines starting from spectral types O5, A3 and about G0. A dotted line parallel to the OB intrinsic colour-colour relation is drawn with an excess $E_{B-V}=0^{m}.38$.

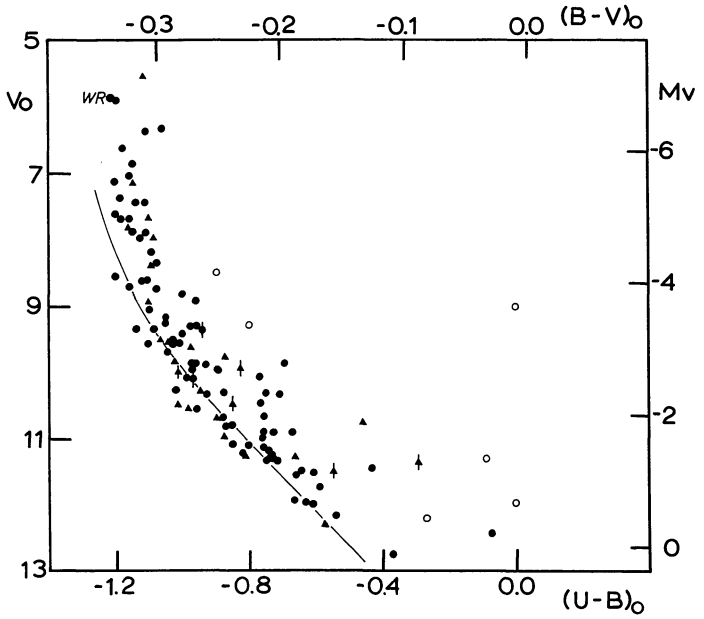

Figure 6 The intrinsic colour-magnitude diagram. The symbols have here again the same meaning as in figure 3. Because for OB stars the relation $(U-B)_0=3.69\ (B-V)_0+0.03$ can be employed the upper and lower margin were labelled accordingly. Vertical bars stand for stars that show variations. The ZAMS with a modulus of $V_0-M_V=12^{m}.65$ is drawn as a full line.

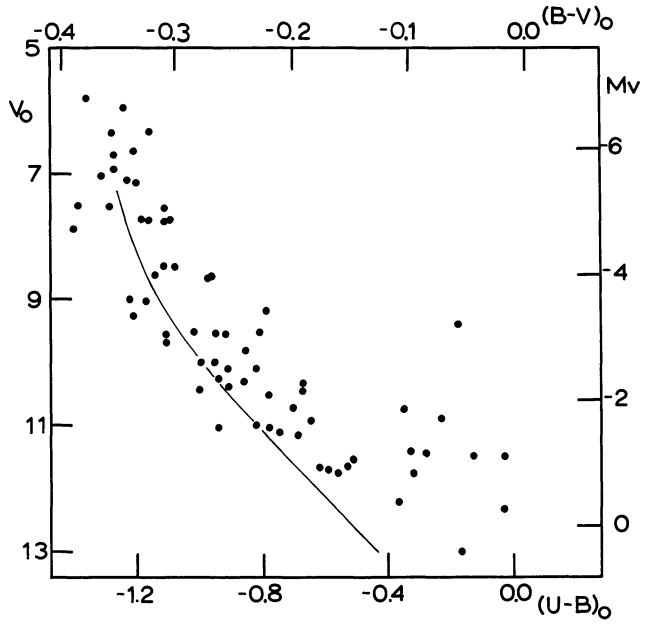

Figure 7 The intrinsic colour-magnitude diagram for NGC 6611 (Walker 1961). This diagram, plotted with Walker's observed data which are reduced in the same way as our data, is shown here for comparison purposes. The modulus for NGC 6611 is $V_o - M_V = 12^m.6$.

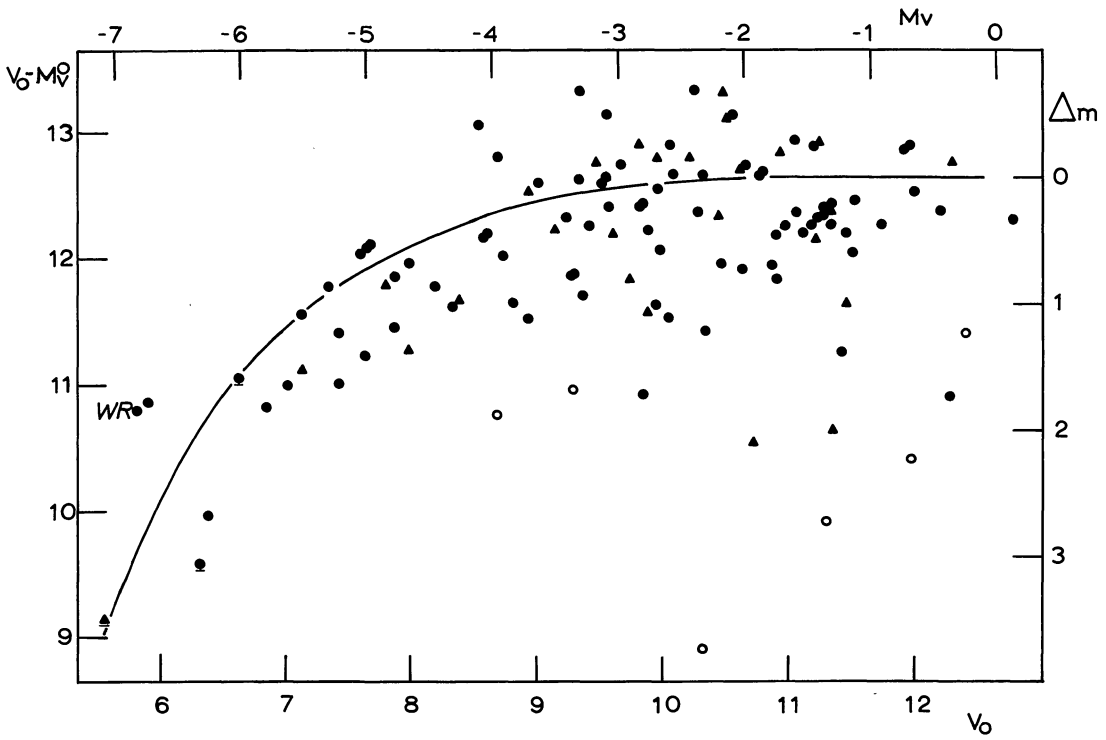

Figure 8 Corrected modulus versus corrected apparent magnitude diagram. The symbols have the same meaning as in figure 3. Binary stars are underlined. The mean evolutionary deviation curve is taken from Lindoff (1968). From the vertical fit a corrected modulus $V_o - M_V = 12^m.65 \pm 0^m.20$ is obtained. The upper margin is labeled in absolute magnitude accordingly.

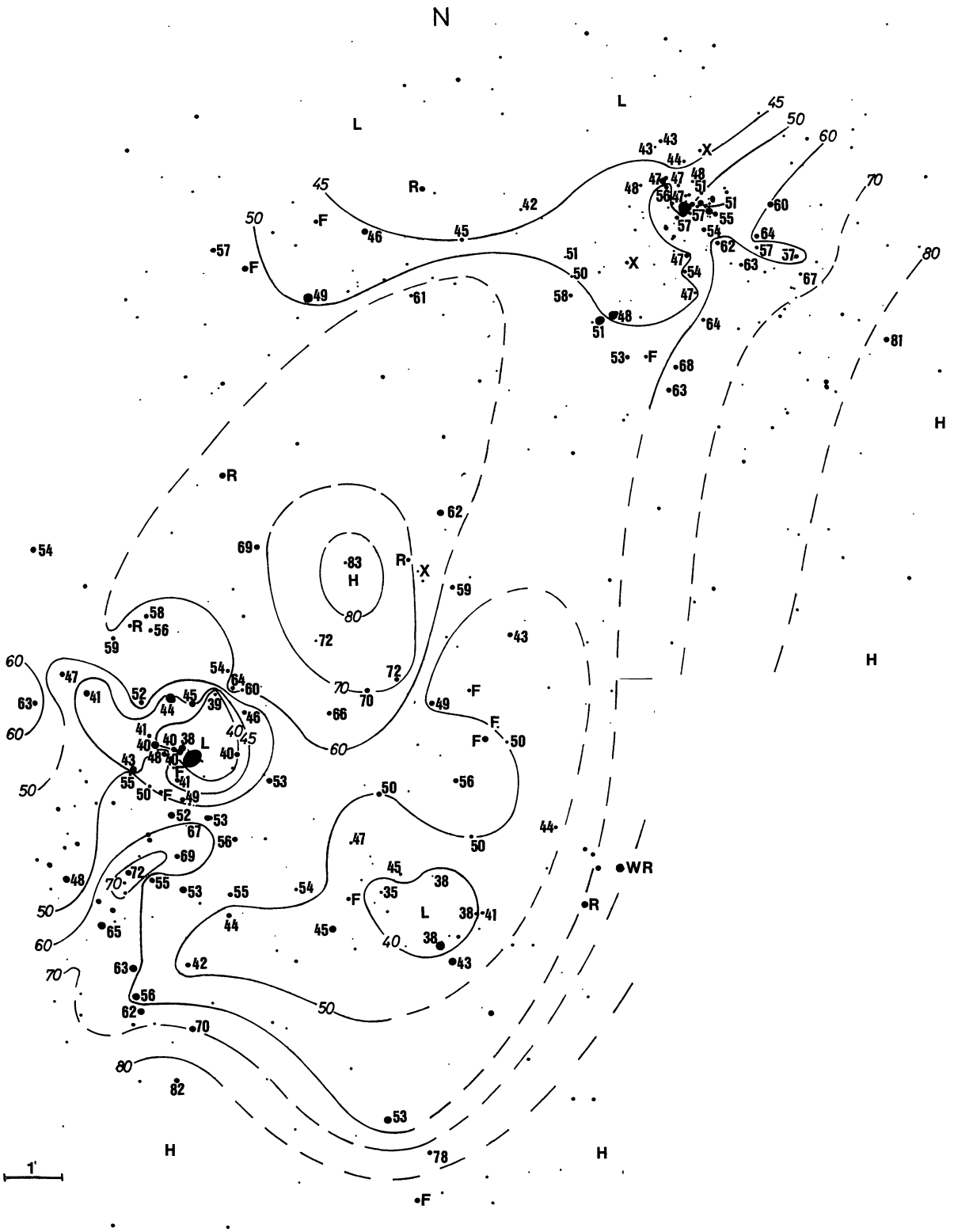

Figure 9 The distribution of the colour excesses for the stars considered to be members of the aggregate is shown as an isocryptic line chart. Each star is labeled with its colour excess expressed in hundreds of magnitude; the isocryptics are labeled in the same way. To stars of which the colour excess are not given the following letters are applied: F, foreground stars; R, red stars; X, stars whose colours are unusual or impossible; WR, Wolf-Rayet star. The isocriptics are drawn as full lines when we can determine them with some confidence. Dashed lines are used only to show a possible way of connecting the whole zone in a coherent picture; they were drawn after inspecting a picture of the region and have only a tentative meaning. H and L denote zones of high and low excess values.

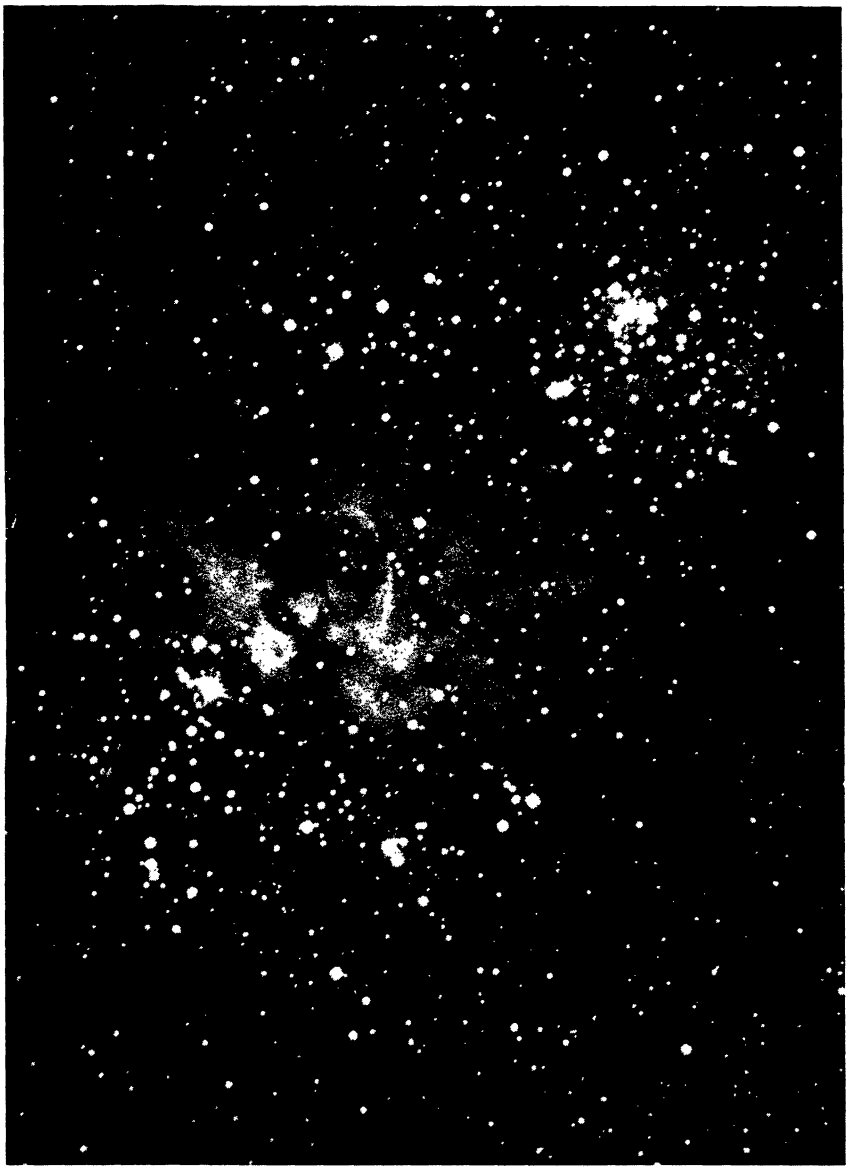

Figure 10 A yellow plate of the η Car region obtained with the Curtiss Schmidt telescope at Cerro Tololo Inter-American Observatory. This plate shows the structure of the bright nebula and is useful for a comparison with figure 9, which gives the distribution of the colour excesses.

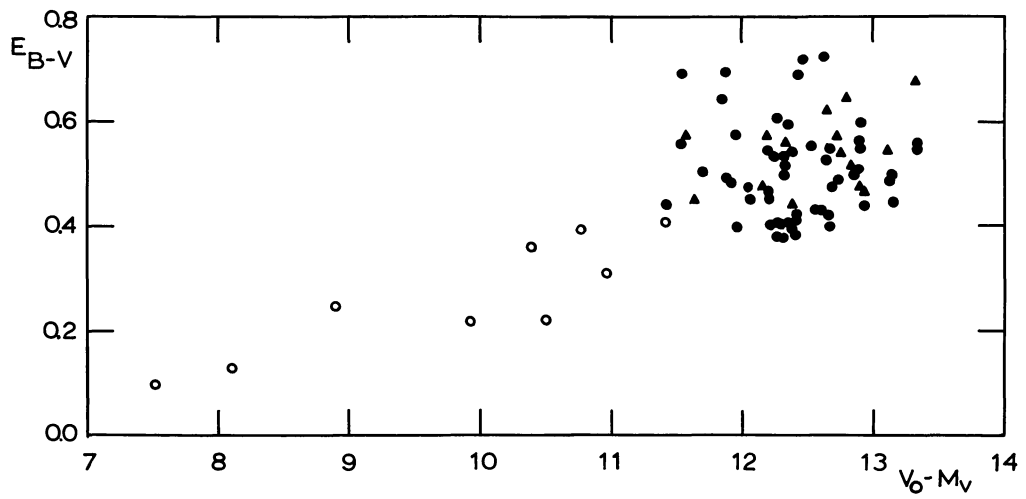

Figure 11 Colour excess versus distance modulus diagram. The same symbols as in figure 3 are used. In order to avoid confusion with those stars having a smaller modulus caused by their evolution, no member stars brighter than $V_0 = 9^m.3$ are included. Also omitted from this diagram are stars nos. 49, 56, 57 of Tr 16 and stars nos. 11 and 15 of Tr 14, because they are located to the right of the main sequence and thus are possibly in the contracting phase.

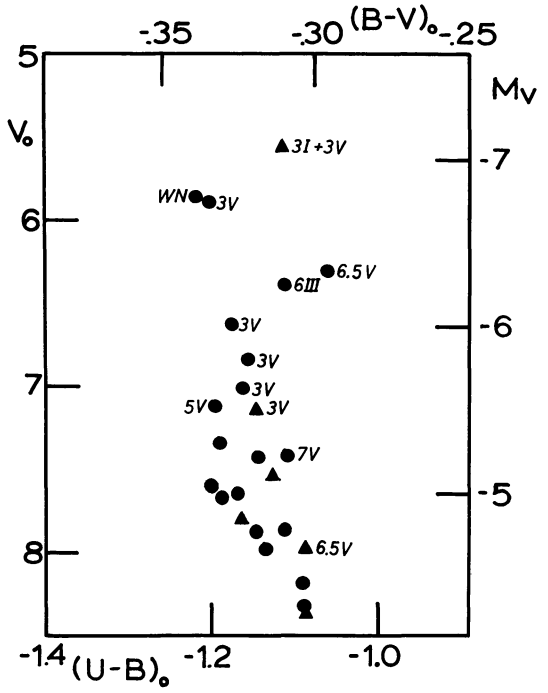

Figure 12 The brightest part of the intrinsic colour-magnitude diagram of figure 6. For the stars with known spectral types they are indicated in the figure without the letter O.

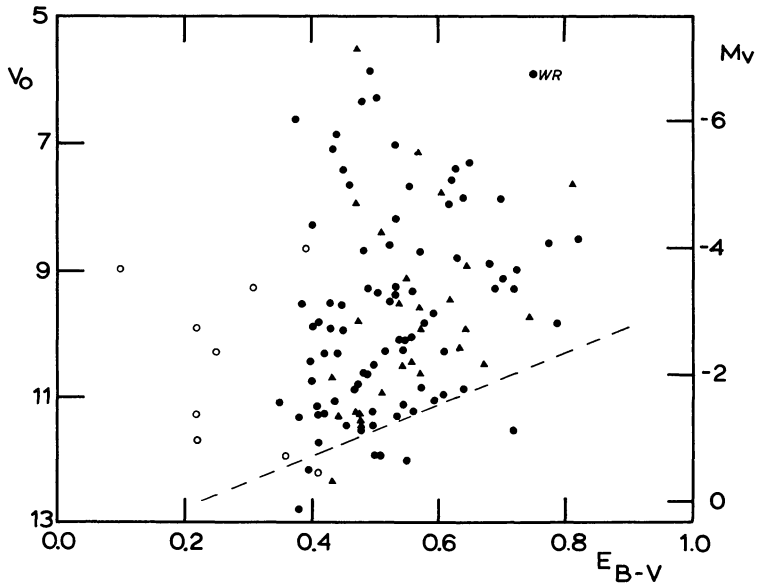

Figure 13 The corrected visual magnitude versus colour excess diagram. The symbols as in figure 3 are employed. The dashed line indicates the observational limit corresponding to $B=13^m.3$ and $A_B/E_{B-V}=4.0$. No correlation such as those suggested by Reddish (1967) is apparent.

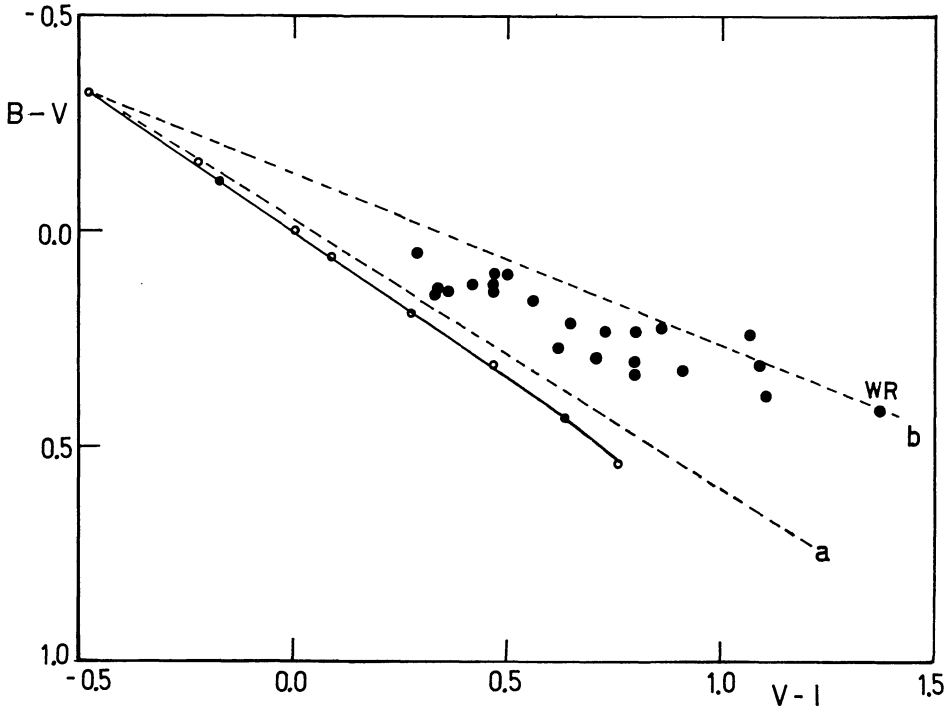

Figure 14 The (V–I, B–V) array for the stars observed in the RI system. The intrinsic colour-colour relation is indicated by a solid line. The two dashed lines indicate the paths for different interstellar reddenings. Line "a" corresponds to $R=3$ and "b" to $R=5$. The position of the interstellar reddening line for the cluster stars is suggested.